Possible hyperdeformed band in ^{36}Ar observed in ^{12}C + ^{24}Mg elastic scattering

Wagner Sciani,* Yul Otani, Alinka Lépine-Szily, Elisangela A. Benjamim,†
Luiz Carlos Chamon, and Rubens Lichtenthäler Filho
Instituto de Física, Universidade de São Paulo, CP 66318, 05389-970 São Paulo, Brazil

Judit Darai
Institute of Experimental Physics, University of Debrecen, HU-4010, Debrecen Pf 105, Hungary

József Cseh
Institute of Nuclear Research of the Hungarian Academy of Sciences, HU-4001, Debrecen Pf 51, Hungary
(Received 12 March 2009; revised manuscript received 28 April 2009; published 24 September 2009)

Fifteen strongly oscillating angular distributions of the elastic scattering of ^{12}C + ^{24}Mg at energies around the Coulomb barrier ($E_{\text{c.m.}} = 10.67$–16.00 MeV) are reproduced by adding five Breit-Wigner resonance terms to the $l = 2, 4, 6, 7$, and 8 elastic S matrix. The nonresonant, background elastic scattering S matrix S_l^0 is calculated using the São Paulo potential. The $J = 2, 4, 6, 7$, and $8\hbar$ molecular resonances fit well into a rotational molecular band, together with other higher lying resonances observed in the ^{16}O + ^{20}Ne elastic scattering. We propose that the presently observed, largely deformed molecular band corresponds to the hyperdeformed band, which has been found previously in α-cluster calculations, as well as in a new Nilsson model calculation. Systematic study of its possible clusterizations predicts the preference of the ^{12}C + ^{24}Mg and ^{16}O + ^{20}Ne molecular structure, in accordance with our present results.

DOI: 10.1103/PhysRevC.80.034319 PACS number(s): 25.70.Bc, 25.70.Ef, 21.60.Fw, 27.30.+t

I. INTRODUCTION

Clusterization, as opposed to a mean-field-like behavior, is an important phenomenon of the atomic nucleus. The best known and most traditional example is that of α clusterization, which is understood as a consequence of the very large binding energy and compact structure of ^{4}He. For similar reasons, heavier α-like nuclei (of equal and even proton and neutron numbers) are also important clusters [1–5]. Recently, evidence of clusterization has been accumulated also in neutron-rich nuclei [5,6].

The interrelation between shape isomers and cluster structure is a long-standing problem. Since the previous ones are usually obtained from shell-model or mean-field calculations, this question leads to the problem of the connection between the different structure models. Several important cluster structures could be associated with the special shapes corresponding to the stable shell structure of the harmonic oscillator potential, while in other cases a molecule-like description is preferred (see, e.g., the reviews [3–6] and references therein). More recent studies [7–10] suggest that there exist (at least) two different phases of clusterization: one is shell-model like, having a simple connection to the shell-model basis; and the other one is the rigid molecule-like clusterization, which can be expressed in terms of shell-model wave functions only in a very complicated way. In the language of the collective model, they correspond to a soft vibrator and a rigid rotor, respectively. Furthermore, they show some similarities to the liquid (shell-like) and solid (rigid molecule-like) phases. They seem to correspond to different (quasidynamical) symmetries, and a quantum phase transition is observable between them [10,11].

The close connection between the clusterization and reaction channel is obvious: from the viewpoint of its observability, a reaction channel defines the cluster configuration [12]. Therefore, reaction studies reveal several interesting aspects of the clusterization. A remarkable example is the appearance of the so-called molecular resonances, found in light heavy-ion reactions. The first and most striking representative of this phenomenon is provided by the ^{12}C + ^{12}C system, in which sharp structures were observed even below the Coulomb barrier [1,13] in the elastic scattering and in reaction channels, with the emission of p, α, n, or γ, or in the fusion and reaction cross-sections. The narrow resonances (width of few hundred keV) were strongly correlated in all channels and presented a very large partial width for decay into ^{12}C + ^{12}C. More recent data [14,15] on the ^{12}C + ^{12}C inelastic scattering indicate that the molecular band terminates with a cluster state of spin $J^\pi = 22^+$ in the compound system ^{24}Mg, at around $E_{\text{c.m.}} = 43$ MeV. Similar resonances were seen in other heavy-ion reactions as well, mainly with α-like nuclei [3–6].

In many light n-α nuclear systems such as ^{16}O + ^{28}Si, ^{12}C + ^{28}Si, ^{16}O + ^{24}Mg, ^{12}C + ^{24}Mg, and others [16], at energies about twice the Coulomb barrier, strong back-angle oscillations were observed in the elastic, inelastic, and α-transfer angular distributions, also called anomalous large angle scattering (ALAS) with large peaks in the excitation functions. Strong correlation between these peaks observed

*Universidade Presbiteriana Mackenzie, São Paulo, Brazil.
†Universidade de Santiago de Compostela, Spain.

in different reaction channels and even in different entrance channels, suggested the interpretation in terms of quasimolecular resonances with two-body clusters in the composed nucleus [4,17].

Alternative interpretations have been put forward for the ALAS in terms of potential calculations, too. Because these phenomena were restricted to n-α nuclei, their interpretation in terms of the coupling between the elastic and the α-transfer channels was a natural step and also gave very convincing results [18–20]. This coupling was represented by a dynamical α-transfer polarization potential, added to the standard optical potential, and could explain the oscillations observed at higher energies, above the Coulomb barrier [18–20].

Another explanation was given by using the double folding optical potential with deep real and shallow imaginary form factors [21] and arguing that the ALAS phenomenon is just due to rainbow maximum. This description reproduces well the ALAS observed in the α-nucleus elastic scattering. However, to reproduce the ALAS phenomenon observed in heavier $N = Z$ nuclei, the imaginary part of the optical potential has to be extremely anomalously shallow, 1–2% of the real depth, not only on the surface but also in the nuclear interior, where the wave functions can penetrate without being absorbed.

In this paper, we analyze the $^{12}C + {}^{24}Mg$ elastic scattering data. The complete set of 15 elastic scattering angular distributions of the $^{12}C + {}^{24}Mg$ system [22], measured at energies very close to the Coulomb barrier, at $E_{c.m.} =$ 10.67–16.00 MeV, shows strong oscillations and were first reproduced [22,23] by a shallow, energy-dependent, phenomenological optical potential. Calculations including the coupling to the α-transfer channel were also performed, and because of the small transfer cross section at the very low energies, they could not explain the observed oscillations [22]. More recently, many attempts have been made and published to reproduce these data using deep real potentials. To be able to reproduce the elastic and inelastic data, small additional derivatives were added to the deep real potential [24–27], or modified Ginocchio-type potentials were used [28].

The study of the elastic scattering at energies well over the Coulomb barrier has led to the elimination of ambiguities and the determination of gross features of the optical potential [29], resulting in the adoption of deep real potentials. On the other hand, the existence of correlated structures in the excitation functions, measured at different angles and different channels, suggests the presence of quasimolecular resonances.

In a separate paper [30], we describe some new results on the structure of the presently proposed hyperdeformed band, and we also review our recent understanding of the shape isomers of the ^{36}Ar. Their relations to the cluster configurations and reaction channels are also discussed.

The structure of this paper is determined by the steps of the new analysis. First the optical potential and the phase-shift analysis are presented to determine the l values needed for the best fit. Then energy-dependent resonance terms are included in the scattering matrix. The results of these calculations are compared with the available experimental data, i.e., angular distributions and excitation functions.

II. BACKGROUND, OPTICAL MODEL SCATTERING MATRIX S_l^O, AND PHASE-SHIFT ANALYSIS

Fifteen complete elastic scattering angular distributions of $^{12}C + {}^{24}Mg$ were measured between $E_{c.m.} = 10.67$ and 16.00 MeV at the University of São Paulo Pelletron tandem [22]. The angular distributions were measured up to $\theta_{c.m.} = 164^\circ$, and they all show strong oscillations. An angular distribution measured at $E_{c.m.} = 16.53$ MeV by Mermaz and collaborators [31] was also included in our analysis.

The starting point in our calculations was a double-folding, deep optical potential, also called the São Paulo potential (SPP) [32,33], where the Pauli nonlocality results in energy dependence of the potential depth. The angular distributions calculated with this strongly absorbing, deep potential present no oscillations. The imaginary part of the potential has the same form factor as the real part, and the normalizations of the real and imaginary parts, respectively, N_r and N_i were varied in our fit procedures to improve the forward angle fit.

An alternative way of analyzing the data is to use an S-matrix or phase-shift analysis. In this method, the S-matrix elements are varied to minimize the χ^2 parameter of the best fit. Often the result of the search procedure depends on the initial values, and the search is not stable and reliable. A new method developed by Chisté *et al.* [34] explores the fact that the χ^2 distribution is of the fourth degree in the S-matrix elements. All three roots of the scale parameter, corresponding to the minimum χ^2 in its gradient direction, are algebraically determined. This procedure turns out to be stable and allows not only the determination of the S-matrix elements but also of their uncertainties, which usually are not known by other methods.

We have performed phase-shift analysis (Figs. 1 and 2) of our 15 angular distributions using the method described above and using the SPP optical model matrix elements as initial values in the search. Very good fits could be obtained when all matrix elements, with l values from $l = 0$ to $12\hbar$ were allowed to vary in the search procedure. However, in this case, the uncertainty in the matrix elements was excessively high, indicating a large ambiguity, and no conclusion about their contribution could be obtained. We tested the number of l values needed and their region to get the best compromise between the quality of the fit and the uncertainty in the matrix elements. The best compromise was obtained using a window of $l = 6$–$9\hbar$. This result indicates that not only one spin contributes, and probably the oscillations are due to overlapping resonances with different spin values. We present in Figs. 1 and 2 examples of both calculations. Because of ambiguities inherent in this method the results of the phase-shift analysis can give only indications of the l values needed for the best fit.

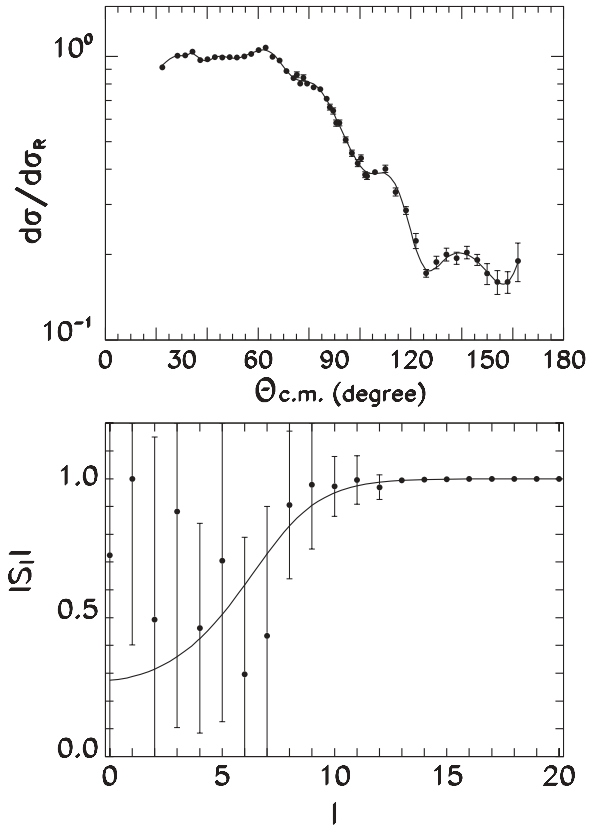

FIG. 1. Phase-shift analysis of the angular distribution of $E_{\text{c.m.}} = 13.00$ MeV, with l values varied between 0 and $12\hbar$. The solid line is the background S matrix, calculated with SPP.

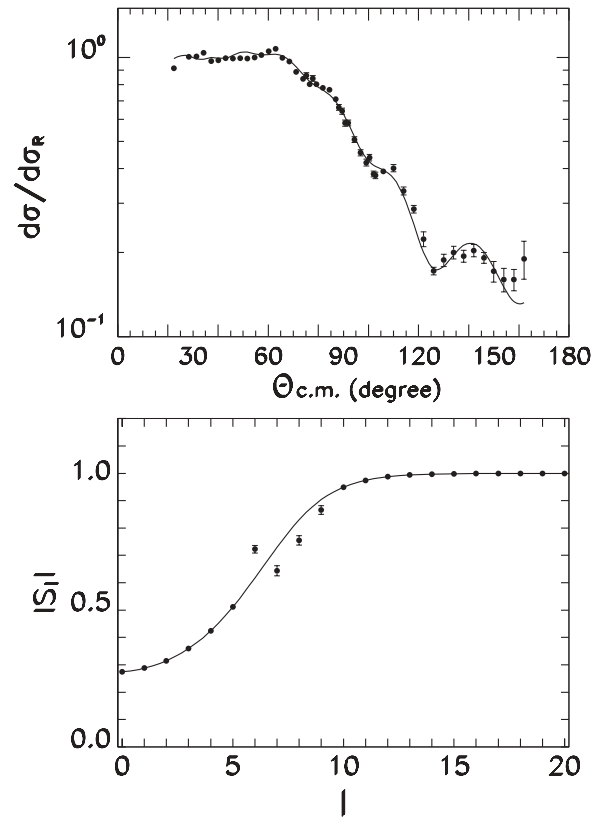

FIG. 2. Same as Fig. 1, but with l values varied between 6 and $9\hbar$.

III. OPTICAL MODEL ANALYSIS INCLUDING ENERGY-DEPENDENT BREIT-WIGNER RESONANCES IN THE S MATRIX

As a first step, we have added Regge poles [35] to the optical model S matrix S_l^o, described above.

$$S_l = S_l^o \left(1 + \frac{i\,De^{2i\Phi}}{(l - l_0) - \frac{i\Gamma}{2}}\right). \tag{1}$$

The angular distributions of $E_{\text{c.m.}} = 13.00, 13.33, 13.67, 14.00, 14.33$, and 14.67 MeV could be well reproduced by a single pole with $l_0 = 6\hbar$ and width $\Gamma = 0.05\hbar$, which means that only the $l = l_0 = 6$ partial wave was affected by the pole. Our interpretation for this is the existence of a $J = 6\hbar$ resonance in the compound nucleus ^{36}Ar at an excitation energy compatible with the corresponding $E_{\text{c.m.}}$. If this resonance had a dinuclear cluster structure of $^{12}\text{C} - ^{24}\text{Mg}$, it could affect the elastic scattering cross section at the corresponding energies. For the angular distributions of $E_{\text{c.m.}} = 15.00$, 15.33, and 15.67 MeV, an $l_0 = 7\hbar$ pole was necessary to obtain a good fit.

The effect of the resonances in the compound nucleus ^{36}Ar was described by adding the energy-dependent Breit-Wigner resonance term $S_{l_r}^{\text{res}}$ to the $l = l_r$ element of the background optical model S-matrix S_l^o, which has a maximum perturbation at $E_{\text{c.m.}} = E_r$ for each resonance r.

$$S_{l_r}(E) = S_{l_r}^o + S_{l_r}^{\text{res}}(E) = S_{l_r}^o - \frac{i\,D_r e^{2i\phi_r}}{(E - E_r) + \frac{i\Gamma_r}{2}}. \tag{2}$$

We associate these resonances to reaction processes that are not included in the optical model S matrix but still contribute to the elastic scattering. The inclusion of the resonance term in the scattering matrix S_l in Eq. (2) is identical or similar to different expressions that have been used in data analysis of other works (e.g., Refs. [36–40]). D_r is the amplitude of the resonant process, contributing to the elastic channel, also called the elastic width. Γ_r is the total width, and E_r is the resonant energy. ϕ_r is the relative phase of the mixing between the background and the resonant process, both contributing to the elastic channel. In some works, the resonant term is multiplied by S_l^o [40], the optical S matrix; in others, by a term that involves only the phase of S_l^o [38,39]. As in Ref. [36], we did not perform this multiplication, which would produce a spurious effect of the resonating term in an energy region quite far away from E_r. In fact, in our case, S_l^o can have a quite large variation in the complete bombarding energy range studied; however, in the energy range of the resonance, Γ_r, the variation of S_l^o is much smaller. Within our assumption, considering a simple sum, the effect of the resonance on the cross sections is restricted to an energy region $\pm\Gamma_r$ around E_r. Anyway, the multiplication cited above would affect mainly the parameters D_r and ϕ_r. For the purpose of our analysis (determination of a rotational band in ^{36}Ar), the most important parameters to be determined are l_r and E_r, which, as we will see, allow the

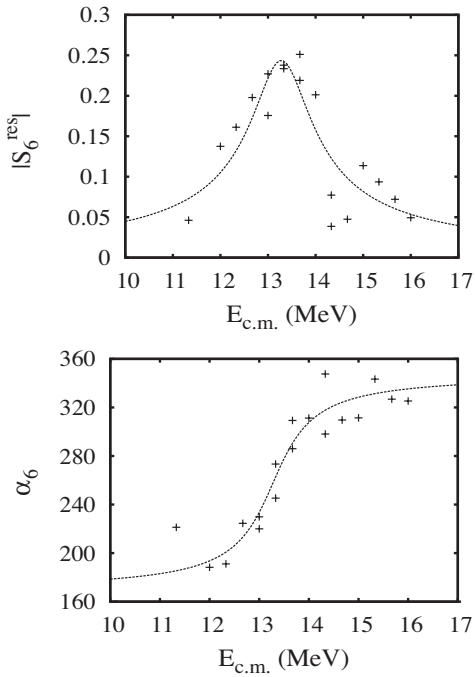

FIG. 3. Top: Energy dependence of moduli of the best fit matrix elements $|S_6^{res}|$ fitted by the Breit-Wigner function. Bottom: Energy dependence of the best fit arguments α_6 (deg) is fitted.

evaluation of the spin and excitation energy of states associated to the hyperdeformed band in ^{36}Ar.

The angular distributions at $E_{c.m.} = 13.00$, 13.33, 13.67, 14.00, 14.33, and 14.67 MeV could be well reproduced by a single pole with $l_r = 6\hbar$. We assumed, to begin with, the existence of only one resonance, represented in the $l_r = 6$ matrix element by $S_6^{res} = |S_6^{res}|e^{i\alpha_6}$ to fit the angular distributions at these energies. In the fit procedure, the χ^2 minimization was realized by a Monte Carlo/C++ code, named POLODSA [41], which uses the downhill simplex annealing algorithm [42]. We performed the parameter search for $|S_6^{res}|$ and α_6 minimizing the χ^2 for each angular distribution at the energies $E_{c.m.}$ mentioned above. The results for $|S_6^{res}|$ and α_6 as a function of $E_{c.m.}$ are presented on the Fig. 3.

The modulus of the matrix element $|S_6^{res}|$ shows a peak as a function of the energy. This peak was fitted by the Breit-Wigner function, determining the parameters $E_6 = 13.21$ MeV, $D_6 = 0.1624$, and $\Gamma_6 = 1.3$ MeV. The energy dependence of the argument α_6 can also be seen on Fig. 3, and the phase parameter $\phi_6 = 127.8^\circ$ could be determined from it. The energy variation of the argument α_6, increasing by 180° at the resonance energy E_6, constitutes a strong indication for the existence of a $J = l_r = 6$ resonance at E_6.

Once the four parameters of the $l_r = 6$ resonance were determined, we repeated the method including the $l_r = 6$ resonance in our S matrix and representing the $l_r = 7$ resonance by $S_7^{res} = |S_7^{res}|e^{i\alpha_7}$. We performed the parameter search for the angular distributions at $E_{c.m.} = 15.0$, 15.33, 15.67, and 16.0 MeV for $|S_7^{res}|$ and α_7, using our best fit code and minimizing the χ^2.

Again the modulus of the $l_r = 7$ matrix element presents a peak as a function of the energy, and its parameters ($E_7 = 15.396$ MeV, $D_7 = 0.0893$, $\Gamma_7 = 1.169$ MeV) were determined by fitting it with the Breit-Wigner function. The phase of the resonance ($\Phi_7 = 79.3^\circ$) could be obtained from α_7, but the precision of the result was worse than in the $l = 6$ case, due to a larger spread in the best fit results. After the inclusion of the $l_r = 7$ resonance, the parameter search for the $l_r = 6$ matrix elements was repeated, and the new values were very close to the values previously determined. The procedure was also repeated for the $l_r = 7$ matrix elements for the ten angular distributions.

The four angular distributions at $E_{c.m.} = 11.33$, 12.00, 12.33, and 12.67 MeV were not well reproduced by the inclusion of the $l_r = 6$ and 7 resonances. The inclusion of an additional resonance at lower energy was necessary, and a search was performed to determine which l_r value would be most appropriate. The lowest χ^2 value was found for $l_r = 4\hbar$, but the inclusion of a $l_r = 5\hbar$ resonance would also improve the fits. We did not include both so as to not increase the number of free parameters unnecessarily.

The same method was repeated, and again the modulus of the matrix element $|S_4^{res}|$ presented a peak, which could be fitted by a Breit-Wigner function. The values of $E_4 = 11.42$ MeV, $D_4 = 0.1927$, $\Gamma_4 = 1.22$ MeV, and $\phi_4 = 79.11$ MeV were determined.

The fit for the two lowest energies $E_{c.m.} = 10.67$ and 11.33 MeV was significantly improved when we included an $l_r = 2\hbar$ resonance also. However, the precision of the determination of its parameters was poor, since it is situated at the edge of the range of energies. Its overall phase could not be determined, and we used the best fit phases obtained for each energy in our calculations.

In our analysis, the angular distribution measured at $E_{c.m.} = 16.53$ MeV [31] was not well reproduced by the inclusion of the $l_r = 2$, 4, 6, and $7\hbar$ resonances in the S matrix.

The inclusion of an additional resonance at higher energy was necessary, and a search was performed to compare $l_r = 8$ and $9\hbar$ for all angular distributions. The lowest χ^2 value was found for $l_r = 8$. The inclusion of $l_r = 9$ gave a better result for the angular distribution of $E_{c.m.} = 16.53$ MeV, but worse for the other neighboring angular distributions. For this reason, we included a resonant term in the $l_r = 8$ matrix element of the form $S_8^{res} = |S_8^{res}|e^{i\alpha_8}$ for all angular distributions between $E_{c.m.} = 10.67$ and 16.53 MeV. However, the l_r value of this resonance is less certain then the previous ones. The same method was repeated, and again the modulus of the matrix element $|S_8^{res}|$ presented a peak, which could be fitted by a Breit-Wigner function. The values of $E_8 = 16.18$ MeV, $D_8 = 0.1208$, $\Gamma_8 = 2.12$ MeV were determined. The phase could not be determined, since again this resonance was situated at the edge of the energy range, and we used the best fit phase for each angular distribution. In Fig. 4 we present, as examples of the quality of the fits, six of the 16 angular distributions and the result of our calculations adding the five Breit-Wigner resonant terms with $l_r = 2$, 4, 6, 7, and $8\hbar$ to the optical model S matrix.

In Table I, we present the parameters of the five resonances obtained from the analysis described in detail above. In

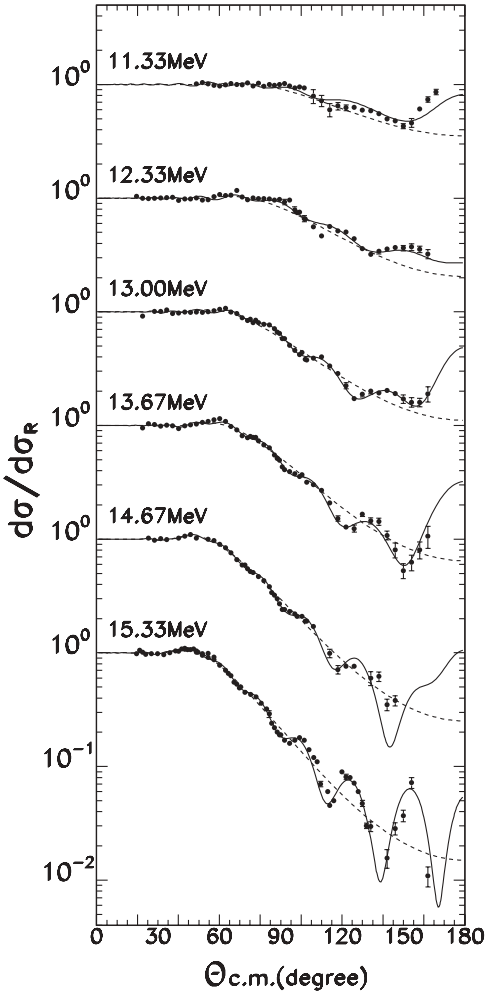

FIG. 4. Angular distributions at $E_{\text{c.m.}} = 11.33$, 12.33, 13.00, 13.67, 14.67, and 15.33 MeV with calculations using SPP (dashed line) and with calculations adding the five Breit-Wigner form resonances $S_{l_r}^{\text{res}}$ to the optical model S-matrix elements (solid line).

Fig. 5, we show the modulus of the S matrix obtained at $E_{\text{c.m.}} = 13.00$ MeV, with and without the inclusion of the five resonances.

The excitation functions of the elastic and inelastic scattering of ^{12}C + ^{24}Mg were measured by Mermaz *et al.* [31] at $\Theta_{\text{c.m.}} = 180^\circ$ between $E_{\text{c.m.}} = 12$ and 26 MeV. In the energy range of our interest, strong peaks are observed at 13.5,

TABLE I. Resonance parameters [Eq. (2)] obtained from χ^2 minimization procedure of the 16 angular distributions of the ^{12}C + ^{24}Mg elastic scattering, as described in the text.

l_r	D_r (MeV)	Φ_r (deg)	E_r (MeV)	Γ_r (MeV)
2	0.0900	∼50.00	10.851	0.595
4	0.1927	79.11	11.420	1.220
6	0.1624	127.8	13.210	1.300
7	0.0893	79.33	15.396	1.169
8	0.1208	∼110.0	16.180	2.120

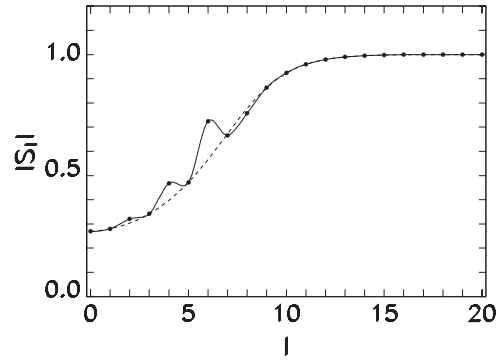

FIG. 5. Modulus of the S matrix obtained at $E_{\text{c.m.}} = 13.00$ MeV, with (solid line) and without (dashed line) the inclusion of the five resonances.

15.5, and 16.5 MeV with width of about 1 MeV. Notice that these energies are close to the energies of the $J = 6$, 7, and $8\hbar$ resonances, $E_6 = 13.2$, $E_7 = 15.4$, and $E_8 = 16.2$ MeV, determined in our analysis of the 16 angular distributions.

In Fig. 6, we compare the excitation function measured at 180° in our energy range [31] with the results of our calculations at the same angle, adding the five Breit-Wigner form resonances $S_{l_r}^{\text{res}}$ to the background optical model S-matrix elements [see Eq. (2) and Table I]. We calculated the cross section only at the energies where we had fitted the angular distributions (10.67, 10.33, 12.00, etc., MeV) since the phases of the resonances with $J = 2$ and 8 were determined only at these energies. There is a qualitative agreement between the calculation and the data, the positions of the peaks are reproduced, but the difference in absolute values can be a problem in the relative normalization between our angular distributions and the excitation function of Ref. [31].

IV. HIGHLY DEFORMED MOLECULAR BAND IN ^{36}Ar

We interpret the five resonances (see Table I) added to the S matrix in our analysis, which reproduce and explain the strongly oscillating angular distributions of the elastic scattering of ^{12}C + ^{24}Mg between $E_{\text{c.m.}} = 10.67$ and 16.5 MeV, as

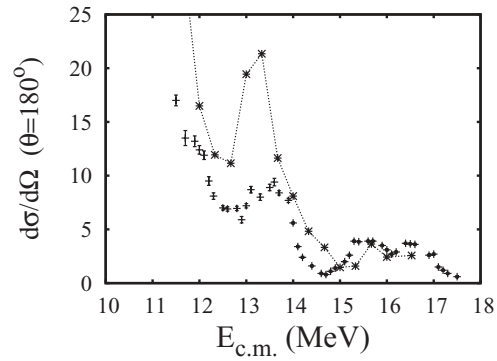

FIG. 6. Excitation functions of the elastic scattering of ^{12}C + ^{24}Mg [31] at $\Theta_{\text{c.m.}} = 180^\circ$ (crosses) with our calculations adding the five Breit-Wigner form resonances $S_{l_r}^{\text{res}}$ to the optical model S-matrix elements (stars).

molecular resonances with dinuclear cluster structure in the ^{36}Ar compound nucleus. As a matter of fact, their resonance energies correspond closely to the energies of the peaks observed in the excitation function measured at 180° [31].

The excitation functions of the elastic and inelastic scattering of ^{12}C + ^{24}Mg [31] present strong structures at the energies: $E_{\text{c.m.}} = 13.5$, 15.5, 16.53, 18.47, 19.07, 20.8, 23.20, and 25.0 MeV. Statistical analysis of the data yielded autocorrelation and cross-correlation functions, which gave a coherence width of FWHM = 0.71 MeV, and cross-correlation coefficients that were rather high. These results supported the presence of intermediate structures.

In Ref. [31], elastic scattering angular distributions were also measured at energies that correspond to the peaks observed in the excitation function, and a phase-shift analysis of the angular distributions was performed. Their conclusion was that good fits could only be obtained when including contributions from many l values.

They fitted the angular distribution at $E_{\text{c.m.}} = 16.53$ MeV by adding two Regge poles with $l_0 = 7$ and 9 to the background scattering matrix. This indicates the presence of an additional $J = 9$ resonance around 16.5 MeV, but we do not have enough data to determine its position or width.

We also performed an analysis of their angular distributions adding two Regge poles [see Eq. (1)] to the background scattering matrix and could obtain quite good fits to the angular distributions with the following l_0 values: for $E_{\text{c.m.}} =$ 18.47 MeV, we added $l_0 = 8$ and 13. For the angular distribution at $E_{\text{c.m.}} = 20.8$ MeV, we added $l_0 = 11$ and 15; and for $E_{\text{c.m.}} = 23.2$ MeV, we added $l_0 = 14$ and 16. We can conclude that the angular distributions are affected by several l_0 values; and as the energy increases, higher l_0 have to be included. However, we can also conclude that for each new energy value the addition of a new l_0 value can be attributed: $l_0 = 9$ for $E_{\text{c.m.}} = 16.5$ MeV, $l_0 = 13$ for $E_{\text{c.m.}} = 18.47$ MeV, $l_0 = 15$ for $E_{\text{c.m.}} = 20.8$ MeV, and $l_0 = 16$ for $E_{\text{c.m.}} =$ 23.2 MeV.

In the γ-ray yield function for the ^{12}C + ^{24}Mg reaction [43] broad oscillations were observed in some channels at $E_{\text{c.m.}} = 18$, 20.5, and 23 MeV. They could be the same states as those later observed in the ^{12}C + ^{24}Mg elastic scattering at $E_{\text{c.m.}} = 18.47$, 20.8, and 23.2 MeV [31].

Shimizu *et al.* [44] measured the excitation function and several angular distributions of the ^{16}O + ^{20}Ne elastic, inelastic scattering and of the ^{20}Ne(^{16}O,^{12}C)^{24}Mg α-transfer reaction between $E_{\text{c.m.}} = 22$ and 39 MeV. Strong correlated structures were observed in the excitation functions at $E_{\text{c.m.}} =$ 24.5, 27.9, 31.7, and 35.5 MeV. Angular distributions of the α-transfer reaction were measured between 10° and 60° at these energies, and they presented strong oscillations. They were fitted using Legendre polynomials with l values of 18, 20, 22(23), and 24(25), respectively.

Gai *et al.* [45] also studied the elastic scattering of ^{16}O + ^{20}Ne between $E_{\text{c.m.}} = 10$ and 29 MeV and observed correlated and strong structures in the excitation functions at 110°, 126°, 136°, and 146°. The peaks were located around $E_{\text{c.m.}} = 18$ and 24.5 MeV, and the angular distributions measured at 17.4 and 24.7 MeV were fitted with resonances of $J = 12$ and 17, respectively.

Miao *et al.* [46] measured angle integrated excitation functions for the ^{16}O + ^{20}Ne and ^{12}C + ^{24}Mg mass partitions in the energy range of $16.39 \leqslant E_{\text{c.m.}} \leqslant 41.67$ MeV for the elastic, inelastic scattering, and α-transfer reactions leading to several excited final states. Large structures are seen in many channels, and some are strongly correlated. Strongly oscillating angular distributions were measured at $E_{\text{c.m.}} =$ 17.5, 19.7, 22.4, 23.1, 24.7, and 25.8 MeV for the mutual ground-state ^{20}Ne(^{16}O,^{12}C)^{24}Mg transitions and at 28.9 MeV for the inelastic transition. They were reasonably well reproduced by single partial wave $P_l^2(\cos\theta)$ fits. The l values used were 10, 12, 15, 15, 17, 17, and 19, respectively.

We transformed the center-of-mass energies into excitation energy in the ^{36}Ar, adding the energy thresholds of 16.298 and 18.452 MeV for the ^{12}C + ^{24}Mg and ^{16}O + ^{20}Ne systems, respectively. In Table II, we summarize the results on excitation energies $E^*(^{36}\text{Ar})$ in the ^{36}Ar compound nucleus together with probable spin values of the resonances observed in our analysis and in Ref. [31] for the ^{12}C + ^{24}Mg system and in Refs. [44–46] for the ^{16}O + ^{20}Ne system.

As the ^{12}C + ^{24}Mg and ^{16}O + ^{20}Ne systems are asymmetric, odd and even spin values are equally allowed for their states. The resonances compiled in Table II have even and odd spin values as well. To verify if these strong structures could correspond to a rotational band of excited molecular states in the ^{36}Ar compound nucleus, we plotted in Fig. 7 these excitation energies against $J(J+1)$, following the equation

TABLE II. Compilation of results on excitation energies and probable spins of resonances observed in the ^{12}C + ^{24}Mg (elastic scattering) and ^{16}O + ^{20}Ne (elastic, inelastic scattering, and α-transfer reactions) channels. They could correspond to a possible hyperdeformed band with cluster structure in the compound nucleus ^{36}Ar. See text for details.

System	$E_{\text{c.m.}}$ (MeV)	$E^*(^{36}\text{Ar})$ (MeV)	J^π	Ref.
^{12}C + ^{24}Mg	10.85	27.148	2^+	This work
”	11.42	27.718	4^+	”
”	13.21	29.508	6^+	”
”	15.396	31.694	7^-	”
”	16.18	32.478	8^+	”
”	16.53	32.83	9^-	[31]
”	18.47	34.77	13^-	[31], this work
”	20.80	37.10	15^-	”
”	23.20	39.50	16^+	”
^{16}O + ^{20}Ne	24.5	42.952	18^+	[44]
”	27.9	46.352	20^+	”
”	31.7	50.152	$22^+(23)$	”
”	35.5	53.952	$24^+(25)$	”
^{16}O + ^{20}Ne	17.4	35.852	12^+	[45]
”	24.7	43.152	17^-	”
^{16}O + ^{20}Ne	17.5	35.752	10^+	[46]
”	19.7	38.152	12^+	”
”	22.4	40.852	15^-	”
”	23.1	41.552	15^-	”
”	24.7	43.152	17^-	”
”	25.8	44.252	17^-	”
”	28.9	47.352	19^-	”

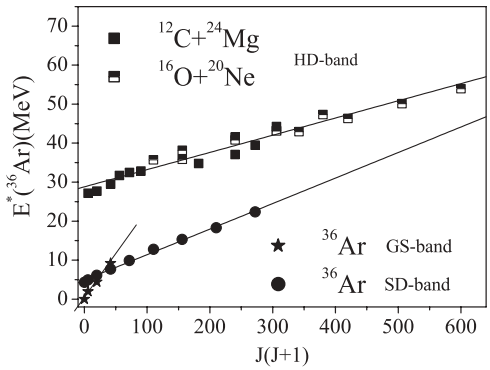

FIG. 7. Excitation energy in ^{36}Ar of the resonances obtained in this work, as well as the resonances observed in the ^{16}O + ^{20}Ne system, as a function of $J(J+1)$. The ground-state and superdeformed bands observed in ^{36}Ar [48] are also included.

below. E_0 is the energy of the bandhead, J is the angular momentum of the resonance, $J = l_r$, and I is the moment of inertia.

$$E^*(^{36}\mathrm{Ar}) = E_0 + \frac{\hbar^2}{2I} J(J+1). \tag{3}$$

The resonances observed in the channels ^{12}C + ^{24}Mg and ^{16}O + ^{20}Ne and compiled in Table II occupy a strip in Fig. 7 with a linear relationship between E^* and $J(J+1)$, indicating that all these states belong to a common rotational band. This band contains states with both positive and negative parity and with even and odd angular momentum, respectively. We performed a linear fit, including all resonances, the low-spin resonances of the ^{12}C + ^{24}Mg system, and also the higher spins and excitation energies of the system ^{16}O + ^{20}Ne (solid line). The bandhead is $E_0 = 28.8(6)$ MeV, and the moment of inertia is $4.4(2) \times 10^5$ MeV fm^2.

If we write the moment of inertia as $I = \mu \times R^2$, where μ is the reduced mass and R is the relative distance, we obtain for the relative distance $R = 7.3$ fm, which is more than double the rms charge radius of the ^{36}Ar, $R_{\mathrm{ch}} = 3.39$ fm [47], indicating a large deformation of the nucleus.

In Fig. 7, we also included the ground-state band and the superdeformed (SD) band, recently observed by Svensson *et al.* [48] in ^{36}Ar. Performing a least-squares linear fit of the SD band, the moment of inertia is $I = 2.97(7) \times 10^5$ MeV fm^2 (solid line in Fig. 7).

Our molecular band (^{12}C + ^{24}Mg and ^{16}O + ^{20}Ne) has a larger moment of inertia than the SD band, thus it is a possible candidate for a hyperdeformed band and is in agreement with the prediction of the α-cluster model [49], as well as with the more recent Nilsson calculations for the shape isomers [30]. The calculated rigid-body moment of inertia corresponding to this shell-model state is 4.21×10^5 MeV fm^2, which approximates the experimental value of 4.4×10^5 MeV fm^2. The preferred clusterizations of this state is that of ^{12}C + ^{24}Mg and ^{16}O + ^{20}Ne [30,50].

For the hyperdeformed band, we have carried out a simple calculation of moment of inertia in terms of rigid, spherical ^{24}Mg and ^{12}C, or ^{20}Ne and ^{16}O clusters, as well. Using the expression for two spheres, with masses M_1 and M_2 and radii $R_1 = r_0 A_1^{1/3}$ and $R_2 = r_0 A_2^{1/3}$, stuck together, their moment of inertia should be $I = \frac{2}{5}(M_1 R_1^2 + M_2 R_2^2) + \mu(R_1 + R_2)^2$, where μ is the reduced mass. We calculated the value of I for the ^{12}C + ^{24}Mg and ^{16}O + ^{20}Ne systems, respectively, using $r_0 = 1.2$ fm and we obtained 4.3×10^5 and 4.6×10^5 MeV fm^2, respectively, a value close to the one observed from the linear fit for the HD band, $I = 4.4(2) \times 10^5$ MeV fm^2.

V. SUMMARY

In this work we have presented a careful analysis of the ^{24}Mg + ^{12}C elastic scattering data. All the available angular distributions around the Coulomb barrier were considered [22]. Energy-dependent Breit-Wigner form resonance terms were considered in addition to the nonresonant background part of the S matrix, which was determined by the São Paulo potential. We have found that the experimental data could be nicely reproduced by taking into account five resonances with spins 2, 4, 6, 7, and 8. These states, together with resonances observed previously in the ^{20}Ne + ^{16}O reactions [44–46], determine a rotational band. Its moment of inertia is very close to that of a hyperdeformed band, provided by α-cluster [49] and Nilsson [30] calculations. The most preferred clusterizations of this band were predicted to be the ^{24}Mg + ^{12}C and ^{20}Ne + ^{16}O binary cluster configurations [50]. Therefore, we propose that the molecular band established by our present analysis corresponds to the hyperdeformed intrinsic state of the ^{36}Ar nucleus.

ACKNOWLEDGMENTS

This work was supported in part by Fundação de Apoio a Pesquisa do Estado de São Paulo (FAPESP) and the Conselho Nacional de Desenvolvimento Cientifico e Tecnologico (CNPq), as well as by the OTKA (Grant No. K72357).

[1] K. A. Erb and D. A. Bromley, in *Treatise in Heavy Ion Science*, edited by D. A. Bromley (Plenum, New York, 1984), Vol. 3.
[2] A. H. Wuosma, Annu. Rev. Nucl. Part. Sci. **45**, 89 (1995).
[3] M. Freer and A. C. Merchant, J. Phys. G **23**, 261 (1997).
[4] R. R. Betts and A. H. Wuosma, Rep. Prog. Phys. **60**, 819 (1997).
[5] W. von Oertzen, M. Freer, and Y. Kanada En'yo, Phys. Rep. **432**, 43 (2006).
[6] M. Freer, Rep. Prog. Phys. **70**, 2149 (2007).
[7] N. Itagaki, H. Masui, and J. Cseh, J. Phys. Conf. Ser. **111**, 012002 (2008).
[8] J. Cseh, P. O. Hess, J. Darai, A. Algora, and H. Yepez-Martinez, J. Phys. Conf. Ser. **111**, 012043 (2008).
[9] J. Cseh, J. Darai, A. Algora, H. Yepez-Martinez, and P. O. Hess, Rev. Mex. Fis. **S54**(3), 30 (2008).
[10] J. Cseh, J. Darai, H. Yepez-Martinez, and P. O. Hess, Int. J. Mod. Phys. E **17**, 2296 (2008).

[11] H. Yepez-Martinez, J. Cseh, and P. O. Hess, Phys. Rev. C **74**, 024319 (2006).
[12] C. Mahaux, Annu. Rev. Nucl. Sci. **23**, 193 (1973).
[13] E. Almquist, D. A. Bromley, and J. A. Kuehner, Phys. Rev. Lett. **4**, 515 (1960).
[14] S. P. G. Chappell, W. D. M. Rae, C. A. Bremner, G. K. Dillon, D. L. Watson, B. Greenhalgh, R. L. Cowin, M. Freer, and S. M. Singer, Phys. Lett. **B444**, 260 (1998).
[15] C. A. Bremner, S. P. G. Chappell, W. D. M. Rae, I. Bostozun, M. Freer, M. P. Nicoli, S. M. Singer, B. R. Fulton, D. L. Watson, and B. J. Greenhalgh *et al.*, Phys. Rev. C **66**, 034605 (2002).
[16] P. Braun-Munzinger and J. Barrette, Phys. Rep. **87**, 209 (1982).
[17] U. Abbondanno and N. Cindro, J. Phys. G **19**, 757 (1993).
[18] R. Lichtenthäler Filho, A. Lépine-Szily, A. C. C. Villari, and O. Portezan Filho, Phys. Rev. C **39**, 884 (1989).
[19] A. Lépine-Szily, R. Lichtenthäler Filho, M. M. Obuti, J. Martins de Oliveira Jr., O. Portezan Filho, W. Sciani, and A. C. C. Villari, Phys. Rev. C **40**, 681 (1989).
[20] A. Lépine-Szily, M. M. Obuti, R. Lichtenthäler, J. M. Oliveira Jr., and A. C. C. Villari, Phys. Lett. **B243**, 23 (1990).
[21] F. Michel, S. Ohkubo, and G. Reidemeister, Prog. Theor. Phys. Suppl. **132**, 7 (1998).
[22] W. Sciani, A. Lépine-Szily, R. Lichtenthäler, P. Fachini, L. C. Gomes, G. F. Lima, M. M. Obuti, J. M. Oliveira, and A. C. C. Villari, Nucl. Phys. **A620**, 91 (1997).
[23] A. Lépine-Szily, W. Sciani, Y. K. Watari, W. Mittig, R. Lichtenthaler, M. M. Obuti, J. M. Oliveira Jr., and A. C. C. Villari, Phys. Lett. **B304**, 45 (1993).
[24] I. Boztosun and W. D. M. Rae, Phys. Rev. C **64**, 054607 (2001).
[25] I. Boztosun, O. Bayrak, and Y. Dagdemir, Int. J. Mod. Phys. E **14**, 663 (2005).
[26] I. Boztosun, Y. Dagdemir, and O. Bayrak, Phys. At. Nucl. **68**, 1153 (2005).
[27] M. Karakoc and I. Boztosun, Phys. Rev. C **73**, 047601 (2006).
[28] G. S. Mallick, S. K. Agarwalla, B. Sahu, and C. S. Shastry, Phys. Rev. C **73**, 054606 (2006).
[29] M. E. Brandan and G. R. Satchler, Phys. Rep. **285**, 143 (1997).
[30] J. Cseh, J. Darai, W. Sciani, Y. Otani, A. Lépine-Szily, E. A. Benjamin, L. C. Chamon, and R. Lichtenthäler, Phys. Rev. C **80**, 034320 (2009).
[31] M. C. Mermaz, A. Greiner, B. T. Kim, M. J. LeVine, E. Muller, M. Ruscev, M. Petrascu, M. Petrovici, and V. Simion, Phys. Rev. C **24**, 1512 (1981).
[32] L. C. Chamon, B. V. Carlson, L. R. Gasques, D. Pereira, C. De Conti, M. A. G. Alvarez, M. S. Hussein, M. A. Candido Ribeiro, E. S. Rossi, and C. P. Silva, Phys. Rev. C **66**, 014610 (2002).
[33] M. A. G. Alvarez, L. C. Chamon, M. S. Hussein, D. Pereira, L. R. Gasques, E. S. Rossi Jr., and C. P. Silva, Nucl. Phys. **A723**, 93 (2003).
[34] V. Chisté, R. Lichtenthaler, A. C. C. Villari, and L. C. Gomes, Phys. Rev. C **54**, 784 (1996).
[35] R. Lichtenthaler and L. C. Gomes, Phys. Rev. C **50**, 3163 (1994).
[36] C. M. Cheng, J. V. Maher, M. S. Chiou, W. J. Jordan, J. C. Peng, W. Oelert, G. D. Gunn, and F. D. Snyder, Phys. Rev. C **20**, 1042 (1979).
[37] D. A. Viggars, T. W. Conlon, F. P. Brady, and I. Naqib, Phys. Rev. C **19**, 2186 (1979).
[38] R. E. Malmin, J. W. Harris, and P. Paul, Phys. Rev. C **18**, 163 (1978).
[39] P. Braun-Munzinger, G. M. Berkowitz, M. Gai, C. M. Jachcinski, T. R. Renner, C. D. Uhlhorn, J. Barrette, and M. J. LeVine, Phys. Rev. C **24**, 1010 (1981).
[40] R. J. Ledoux, M. J. Bechara, C. E. Ordonez, H. A. Al-Juwair, and E. R. Cosman, Phys. Rev. C **27**, 1103 (1983).
[41] R. Kuramoto and E. A. Benjamim (private communication on POLODSA routine).
[42] W. H. Press, S. A. Teukolsky, W. T. Vetterling, and B. P. Flannery, *Numerical Recipes in C: The Art of Scientific Computing*, 2nd ed. (Cambridge University, New York, 1993).
[43] R. M. Freeman, F. Haas, B. Heusch, and S. M. Lee, Phys. Rev. C **20**, 569 (1979).
[44] J. Shimizu, W. Yokota, T. Nakagawa, Y. Fukuchi, H. Yamaguchi, M. Sato, S. Hanashima, and Y. Nagashima *et al.*, Phys. Lett. **B112**, 323 (1982).
[45] M. Gai, G. M. Berkowitz, P. Braun-Munzinger, C. M. Jachcinski, C. E. Ordoñnez, T. R. Renner, and C. D. Uhlhorn, Phys. Rev. C **30**, 925 (1984).
[46] Y. Miao, R. W. Zurmuhle, S. P. Barrow, N. G. Wimer, J. T. Murgatroyd, C. Lee, and Z. Liu, Phys. Rev. C **53**, 815 (1996).
[47] I. Angeli, At. Data Nucl. Data Tables **87**, 185 (2004).
[48] C. E. Svensson *et al.*, Phys. Rev. Lett. **85**, 2693 (2000).
[49] W. D. M. Rae and A. C. Merchant, Phys. Lett. **B279**, 207 (1992).
[50] J. Cseh, A. Algora, J. Darai, and P. O. Hess, Phys. Rev. C **70**, 034311 (2004).